15th International Symposium on Flow Visualization
June 25-28, 2012, Minsk, Belarus

MACH WAVE NOISE OF A SUPERSONIC JET

H. OERTEL SEN.[1], F. SEILER[1,c], J. SRULIJES[2]

[1]Karlsruhe Institute of Technology (KIT), Institute for Fluid Mechanics, D-76133 Karlsruhe, Germany
[2]French-German Research Institute of Saint-Louis (ISL), 68301 Saint-Louis, France

[c]F. Seiler: Tel.: +4972160842368; Fax: +4972160845147; Email: friedrich.seiler@kit.edu

KEYWORDS:
Main subjects: free jet noise, Mach wave generation
Fluid: supersonic free jet, mixing layer, sources of Mach waves, vortex pairs
Visualization method(s): differential interferometry, immobilizations, streak records
Other keywords: wave propagation speeds, three characteristic velocities

ABSTRACT: Supersonic jets emit noise to the outside in form of Mach waves which are long, straight and have about equal angles. Experiments done by Oertel sen. visualized clearly these Mach waves and he publicized moreover that such Mach waves exist also inside the jet. Experimental and theoretical studies in the past did not allow a complete understanding of the phenomenon up to now, wherefore the need for further research is obvious. In this study the observations of Oertel sen. are described and an assumption is given for illuminating theoretically the experimental outcomes. The Mach waves inside and outside are visualized by single frames, by immobilization images and by streak records. Differential interferometry (DI) is used for visualizing density differences by light intensity variations. Measuring the Mach wave angles from many shock tube experiments revealed the existence of three wave families. They move with different speeds, denoted as w, w' and w'', which depend only on the jet Mach number M_i and the ratio a_a/a_i of the sound speed a_a outside and a_i inside the jet. A theory is proposed which explains the three speeds found. Its central point is the production of Mach waves by pairs of vortices moving inside of the jet mixing layer. Each pair is built by a front and a rear vortex. The front vortices create the w'-Mach waves outside the jet and the rear vortices are accompanied by the w''-Mach waves inside. The w-Mach waves go together with the notch in-between both and are finally also formed when a front vortex combines with an overtaking preceding rear vortex, both creating only one big vortex which moves with w. The processes mentioned are mainly suggested by the immobilizations and by the streak records taken. For both the flow is observed through a slit on a rotating drum camera. Immobilizations use a wide opened slit and the camera turns with the speed of the Mach waves to be observed. Streak records show clearly with a narrow adjusted slit the Mach wave traces. The explanations given are only valid for the beginning of a supersonic jet up to about ten jet diameters downstream.

Nomenclature

flow velocity

u = general, u* = special, u_i = inside the jet

propagation velocity

w = centre of vortex pair, w' = front vortex, w" = rear vortex

speed of sound

a = general, a* = special, a_i = jet gas inside, a_a = gas outside

Mach numbers

M_j = jet Mach number, $M_i=u_i/a_i$ = inside the jet with $M_i = M_j$

w/a_a = of the w-Mach wave outside, w'/a_a = of the w'-Mach wave outside

$(u_i-w)/a_i$ = of the w-Mach wave inside, $(u_i-w")/a_i$ = of the w"-Mach wave inside

Mach angles

α = w-Mach wave inside and outside, α' = w'-Mach wave outside, $\alpha"$ = w"-Mach wave inside

other parameter

e = optical beam separation inside the differential interferometer

1 Introduction

A supersonic jet is known as a source of remarkable noise which can become intolerable in the environs of jet engines, cutting torches and other supersonic jet producing devices. The most dangerous part of the noise is emitted in form of Mach waves which provoke short-time pressure variations comparable to shock waves. It is clear that a certain “important order” must exist inside of the jet mixing layer, separating the moving jet gas from the outside gas at rest, which initiate the Mach waves to be formed. They appear inside as well as outside of the jet and are quite regular. The practically ideally expanded supersonic free jet in Fig. 1 shows obviously the outside Mach waves by light and dark backwards inclined traces as visualized by Oertel [1, 2] using a differential interferometer (DI).

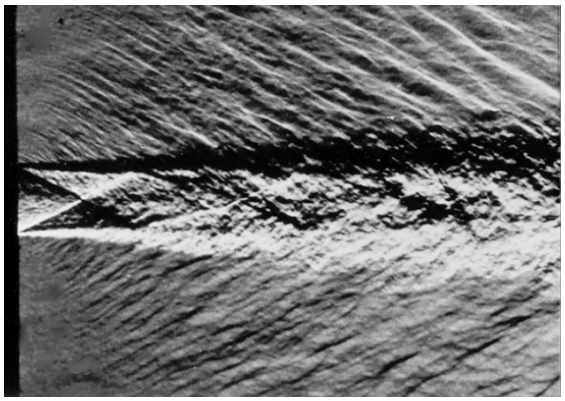

Fig. 1 Mach waves outside of a supersonic Mach number $M_j = 2.65$ free jet with $a_a/a_i = 0.90$

The origin of the Mach waves was attributed to a multitude of different phenomena, as extensively described in the related literature by many authors, see [3-18]. They have been assumed to originate from turbulence as well as from coherent structures of different strong nature. As well some articles suppose that these structures are coupled with eddies which move supersonically downstream inside of the mixing layer. But these studies did not definitely answer the question for the Mach wave initiating mechanism. With studies performed at ISL the kinetics of the Mach wave production was investigated extensively by Oertel sen. [1, 2, 19-25] using a large variety of interferometric visualization techniques based on differential interferometry [25] for visualizing density differences by light intensity variations. The Mach waves inside and outside were observed by single frames (see Fig. 1), by immobilization images (Fig. 2) and by streak records (Fig. 3).

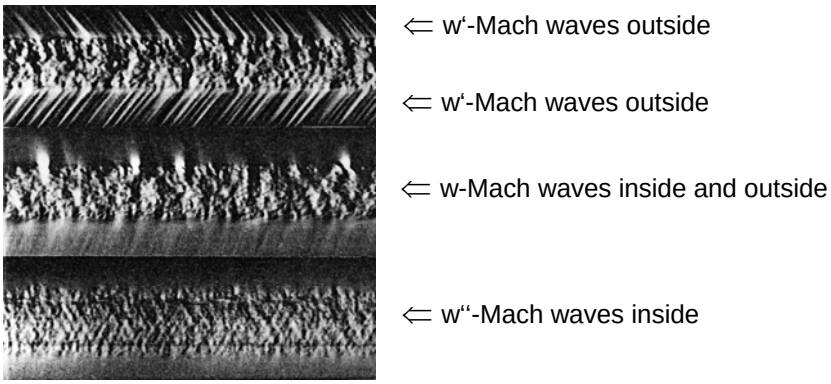

Fig. 2 Immobilizations (vertical y-slit wide open): $M_j \approx 1{,}50$

2 Shock tube operation for jet formation

The experiments were performed with the ISL high energy shock tube STA using different optical methods for jet formation [26]. Fig. 4 represents two of them. Most shock tube measurements have been obtained with the method of shock reflection using well contoured nozzles, see Fig. 4 left. In that case the incident shock wave is reflected at the nozzle throat forming

⇐ w‘‘-Mach waves inside

the stagnation conditions (R) for the nozzle expansion. Some experiments with the non reflected method using the incident shock initiated flow (2) allowed varying the thickness of the exit boundary layer by the length of the tube, see Fig. 4 right.

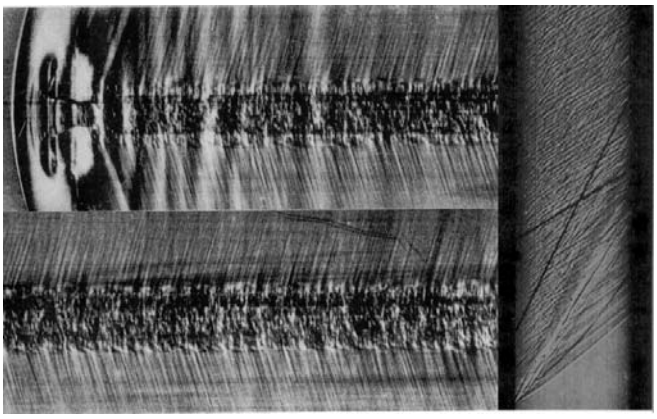

Fig. 3 Streak records at supersonic Mach numbers
left two stapled images with vertical y-slit: $M_j = 2.02$ and $a_a/a_i = 0.97$,
right image with horizontal x-slit: $M_j = 2.20$ and $a_a/a_i = 0.93$

The jets were blown out into a large test vessel with optical access mounted at the end of the shock tube such that both, the pressure and the temperature of the ambient gas, could be controlled. Special care was given to the equality of exit and ambient pressures (≅ 100 kPa). The shock tube experiments are performed at jet Mach numbers $M_j \approx 1.5$ up to 4, most of them at $M_j \approx 2$. Cylindrical as well as slit jets have been studied. The cylindrical ones were produced by nozzles with exit diameters between 1.9 mm and 20 mm. The dimensions of the slit exit were 5 mm x 20 mm.

Fig. 4 Jet productions: reflected mode left, non reflected mode right

2 Optical measuring techniques applied

For visualizing the Mach waves outside of the jet, called w'-Mach waves, the single frame recording technique is used successfully, as obviously seen in Fig. 1 by the Mach wave traces originating from the jet's mixing layer. The Mach waves inside, the w''-Mach waves, can best be detected by immobilization records on moving film inside a drum camera [25] as shown in Fig. 2 for looking with the DI through the hiding turbulence and the Mach waves outside. Naturally the immobilization method was also fruitful applied to visualize the w'-Mach waves outside. In addition to the w'- and the w''-Mach waves there exist a third family which is called w-Mach waves, as well seen profitably by immobilizations. Such records have been used [1, 2, 19 - 24] to make the jet noise emitted able to be seen for determining the three Mach wave speeds, the w-, w'- and w'', by measuring their angles α, α' and α'' against the jet axis.

The optical set-up of the DI is shown in Fig. 5. The light bundle coming from the light source S is, after being linearly polarized by polarizer P1 by 45 degrees to the optical axes of the Wollaston prism W1, separated by W1 into two beam parts crossing parallel the measuring section with a beam separation of about e = 0.1 mm. On the illumination side the lenses OS and O1 make the light beam parallel. On the observation side the two light bundles are transferred by O2, O3 and O4 onto the camera via the aperture A. The second Wollaston prism W2 recombines both light beams and focuses them for individual pictures on a single frame or high-speed camera and for the immobilizations and streak records onto the rotating drum of a drum camera via a $\lambda/4$-plate which makes the two light bundles capable to interfere. The interference is visualized on the camera by light intensity variations which give information on the density gradients along the separation e

between the two light bundles passing the test section. The density gradients are mainly produced by the density change across the Mach waves, as seen on the Figs. 1 to 3 as light and dark lines representing visually the jet's noise emitted.

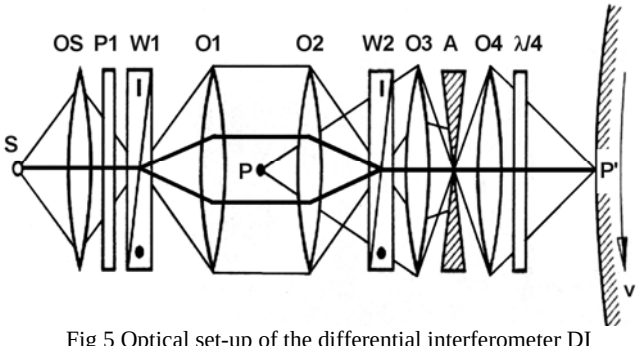

Fig 5 Optical set-up of the differential interferometer DI

For taking immobilizations like those shown in Fig. 2 and the streak records in Fig. 3, for both the flow is observed through a slit on a rotating drum camera. The slit can be arranged in y-direction or in x-direction as depicted in Fig. 6. Immobilizations are taken with a wide opened slit of width sw (Fig. 7) on the camera film rotating with the speed v which is equal to the speed c_x of the moving structures, the Mach waves to be observed. The streak records show clearly with a narrow adjusted slit the Mach wave traces. φ is the angle of the Mach waves on film, γ is the real angle of the jet's Mach waves. Via both slit arrangements, schematically drawn in Fig. 7, the Mach waves are focused as shown in Fig. 8 on the film which is attached to the drum of the drum camera.

The streak records visualize all Mach waves passing a narrow slit like those in Fig. 3 and the angles β are influenced by the streak record velocity; see Fig. 8. On Fig. 3 three streak records are given. The two left stapled streaks are taken with a slit arrangement in y-direction. The upper left shows the beginning of the jet with the jet's head and the lower left the jet's region more downstream. By x-streak registration the Mach wave traces on the right hand side image of Fig. 3 are obtained. They show obviously quite different views of the Mach waves as those taken with the immobilization technique, as seen in Fig. 2. The immobilization opens the window as wide as is necessary for blurring out all details moving in the picture at different speeds from that of the moving film. The film speed here is equal to the speed c_x of the structures to be observed, i.e. if $v = c_x = w$, or w', or w'', the three families of Mach waves are seen on the immobilizations as depicted in Fig. 2 with the three mentioned speeds.

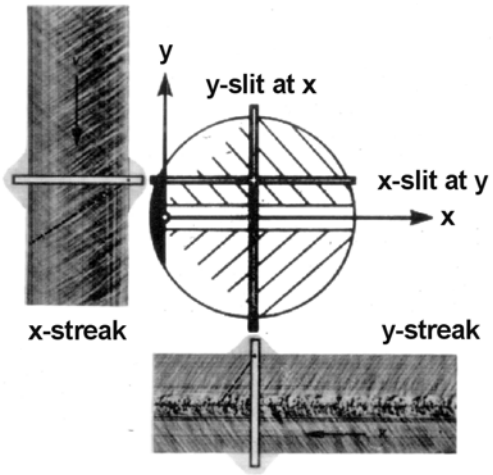

Fig. 6 x-and-y-slit arrangement

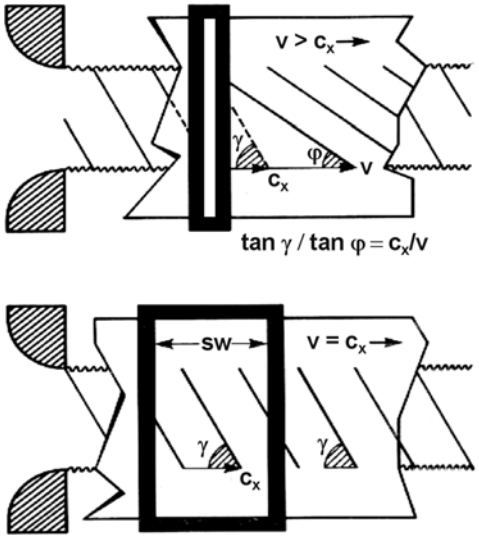

Fig. 7 narrow adjusted (streak record) and wide open slits (immobilizations)

The Mach angles slightly fluctuate due to turbulence. Therefore the evaluation of the Mach angles seen on the flow pictures and consequently the speeds of the Mach wave producing structures, the three w, w' and w'', had to be determined carefully. This has been done by using different independent estimations. The mean value of the three somewhat different angles has been considered to be the result. The evaluation was restricted to equal gases N_2 or air inside and outside the jet.

On images as Figs. 1 and 2, two strong different Mach waves (w and w') can be seen to exist outside the jet as well as two different inside (w and w''). They were found to be produced by "jet boundary layer structures" propagating downstream at the three mentioned speeds. For determining these speeds the following relations were employed, using the measured Mach angles α, α' and α''. The w-Mach waves have equal angles α inside and outside. The w'-Mach waves outside have angle α' and the w''-Mach waves inside have angle α'' as:

$$\sin\alpha = \frac{a_a}{w} = \frac{a_i}{u_i - w} \quad (1),$$

$$\sin\alpha' = \frac{a_a}{w'} \quad (2),$$

$$\sin\alpha'' = \frac{a_i}{u_i - w''} \quad (3).$$

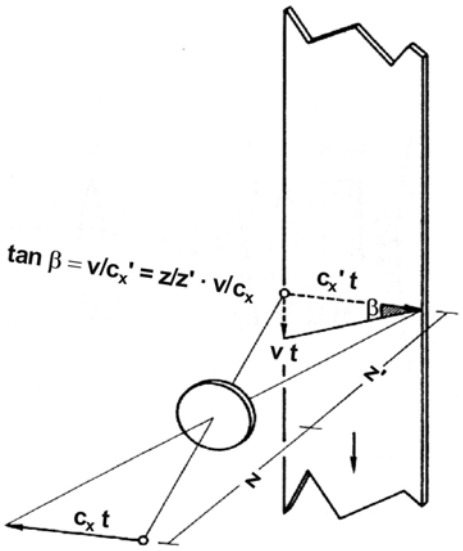

Fig. 8 Focusing on moving film rotating inside a drum camera

Results for the different wave angles obtained from many experiments are shown in Fig. 9. The measured points lie along three straight lines when using on the ordinate the relative Mach number of the Mach wave producing structures seen from inside and normalized with the jet's sound speed a_i. On the abscissa the relative Mach number seen from outside is depicted and is normalized with the sound speed a_a outside the jet. For the fitted straight lines the simple equations (4 - 6) describe the speeds w, w' and w'' very accurately. The three equations (4 - 6) are changed to relations (7 - 9) by introducing the jet flow Mach number $M_i = u_i/a_i$.

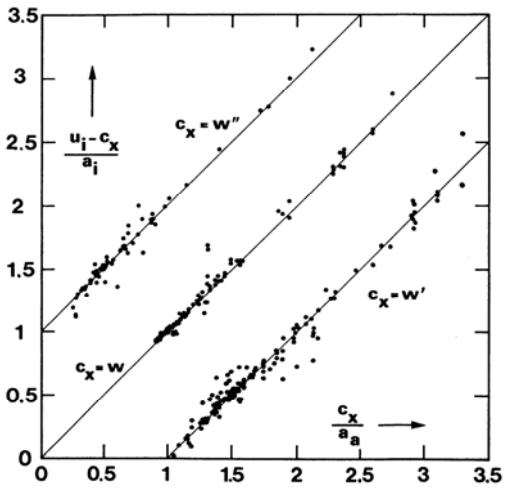

Fig. 9 Experimental results

These equations show apparently that the three speeds simply depend on the jet Mach number M_i and the ratio a_a/a_i of the sound speed outside a_a and inside a_i of the jet.

$$\frac{u_i - w}{a_i} = \frac{w}{a_a} \quad (4) \text{ and } \frac{w}{a_a} = \frac{M_i}{1 + a_a/a_i} \quad (7),$$

$$\frac{u_i - w'}{a_i} = \frac{w'}{a_a} - 1 \quad (5) \text{ and } \frac{w'}{a_a} = \frac{M_i + 1}{1 + a_a/a_i} \quad (8),$$

$$\frac{u_i - w''}{a_i} = \frac{w''}{a_a} + 1 \quad (6) \text{ and } \frac{w''}{a_a} = \frac{M_i - 1}{1 + a_a/a_i} \quad (9).$$

3 Mach waves producing structures

Some older [e.g. 5] and many recent publications [e.g. 13, 14] assume that vortices are formed inside of the mixing layer and are the source for the Mach wave emission. The experiments done by Poldervaart and Wijands [5] demonstrated that vortex pairs might be the origin of the Mach waves. They took shadowgraphs on photos of a much larger, colder and longer blowing supersonic jet than that considered here. Periodic spark shock waves were used for creating successive vortex pairs in the jet's mixing layer. Fig. 10 shows a picture series from [5] with the supersonic jet and the downstream moving vortices. By cutting such a video sequence of Poldervaart and Wijands the speed of displacement became visible as depicted in Fig. 10. It is found that the middle of the vortex pair displaces with the velocity w which is specified in equation (10) as the speed of a deformation shaped by a Kelvin-Helmholtz-Instability. The shadowgraphs show the vortex flow field from a density point of view and on the shadow pictures typical snake-like lines are seen representing the vortex pairs formed. Similar snake-like structures are also seen in the publication of Freund et al. [16] on visualized numerical results at the beginning of the jet mixing layer of a supersonic jet.

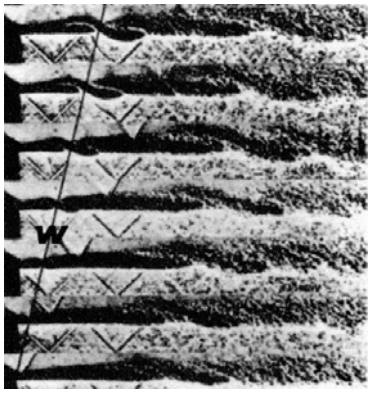

Fig. 10 Picture arrangement from [5]

Rossmann et al. [17] describe strong shocks on both sides of a mixing layer at supersonic jet conditions. They found two different propagation speeds inside the mixing layer which must be associated with "fast- and slow-mode structures", which travel in different transverse locations within the shear layer. It is apparent from the Rossmann et al. paper that they believe these structures are formed by eddies.

Shock tube experiments with a jet produced with the reflected shock tube mode (see Fig. 4) at a jet Mach number 2 visualized the behaviour of smoke particles in the jet's mixing layer [27]. A thin light sheet illuminates the smoke tracers seeded inside and outside the jet. The scattered light observed shows clearly the mixing layer well established in Fig. 11 and reveals black regions. Each of them may represent the combined centers of two vortices where the smoke has been centrifuged out and sucked away.

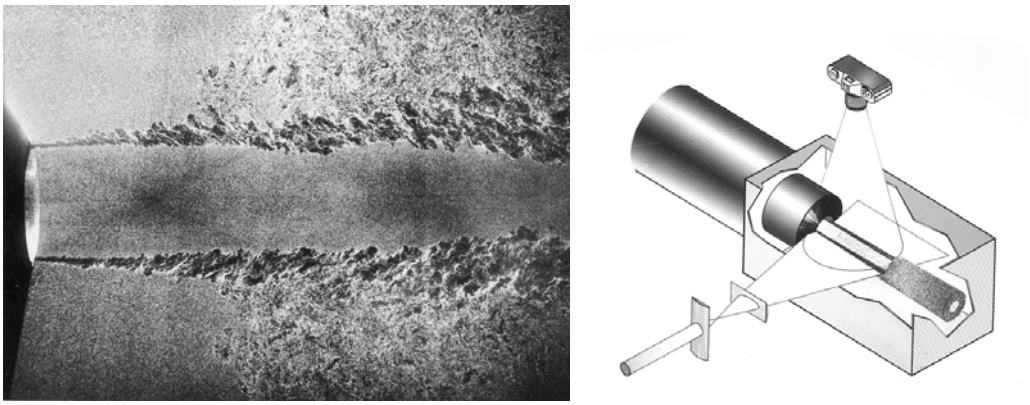

Fig. 11 Mach 2 jet seeded with smoke particles

4 Deduction of the three velocities w. w' and w''

In some experiments of Oertel [2] a very thin jet boundary layer developed for a short distance after the jet's exit which could be considered as a shear layer deformation as shown in Fig. 12. The behavior of the introduced deformation depends on the Mach number M = u/a being higher or lower than one. For estimating the deformation behavior in supersonic as well as in subsonic flow regimes basic knowledge is needed about compressible flows over wavy walls.

The pressure increases in converging and decreases in diverging supersonic flow. The deformation acts on either side like a bump, consisting of a concave indentation followed by a convex bulge. Both the underpressures within the indentations and the overpressures on the bulges contribute to the damping and final disappearance of the deformation.

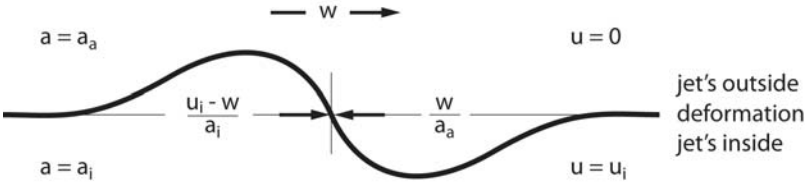

Fig. 12 Deformation of the shear layer

The pressure decreases in converging and increases in diverging subsonic flow. Now the deformation is not damped but grows until the Kelvin-Helmholtz-Instability makes it rolling up into two vortices forming a vortex pair which moves downstream inside the mixing layer. A vortex pair is shown schematically in Fig. 13 with a vortex in front and one at the back, both moving in separate zones. It may happen that further downstream the rear vortex of a vortex pair growth together with the front vortex of a preceding vortex pair which finally disintegrates into turbulence more downstream. Freund et al. [16] and Oertel sen. [2, 19 - 24] found that the Mach waves are highly three dimensional with a short azimuthal correlation. In consequence the vortex pairs are as well only correlated at short distances to each other.

The speed of the shear layer deformation is denoted as w. In order the deformation remains point symmetric, for stability reasons the pressures at both sides must be equal which requires equality of the relative Mach numbers of the two opposite flows in the frame moving with w as:

$$\frac{u_i - w}{a_i} = \frac{w}{a_a} \quad (10) \quad \text{and} \quad \frac{w}{a_a} = \frac{M_i}{1 + a_a/a_i} \quad (11).$$

Similar considerations are assumed to be allowed for the two vortices of the vortex-pair mentioned and shown schematically in Fig. 13 for one vortex-pair moving downstream inside the mixing layer. In the case of laminar exit boundary layer, vortex pairs arise somewhat downstream by Kelvin-Helmholtz-Instability of the layer deformations. When the boundary layer is already turbulent, the vortex pairs are generated immediately at the exit. The instantaneous lines of equal densities may be close to elliptic like those seen in Poldervaarts shadowgraphs [5], see Fig. 10, but are shown here for simplicity as circles. The two vortices rotate around the same angle direction. For reasons to be explained, they remain in different zones of the mixing layer. The centre of the frontal vortex moves downstream with speed w'. It moves within the inner zone and produces a weak shock wave called w'-Mach wave outside the jet. The centre of the rear vortex moves downstream with speed w''. It moves within the outer zone and produces a weak shock wave called w''-Mach wave inside the jet. Intrusion out of his zone would expose each of the vortices to rising pressures caused by the Mach waves which force the vortices to stay and displace stabile in different zones.

T is

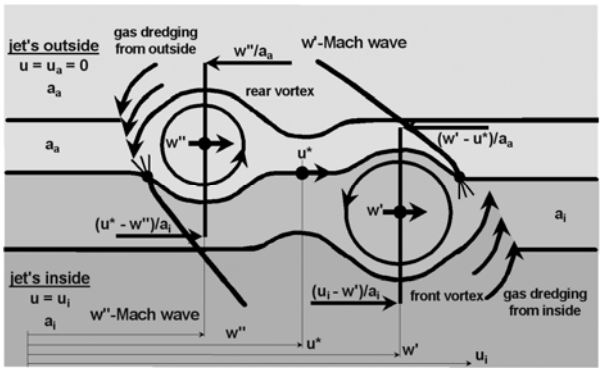

Fig. 13 Vortex pair formed inside the mixing layer

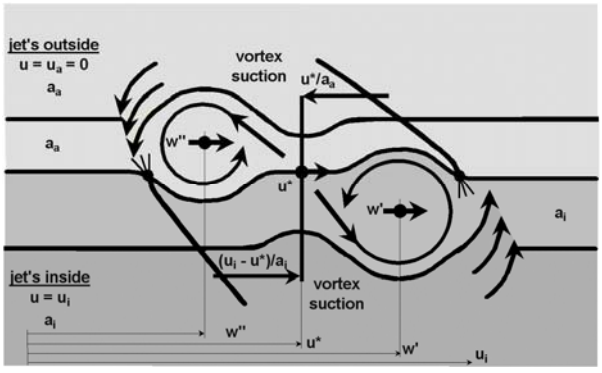

Fig. 14 Sucking action of the vortex pair

Writing the equilibrium conditions for the two vortices within two frames moving at their quite different speeds w' and w'', in the w'-system the opposite subsonic flows over the front vortex and in the w"-system over the rear vortex produce equal pressures at the following equal Mach numbers:

$$\frac{u_i - w'}{a_i} = \frac{w' - u^*}{a_a} \quad (12) \quad \text{and} \quad \frac{u^* - w''}{a_i} = \frac{w''}{a_a} \quad (13).$$

These considerations would only be valid just at the beginning of the jet. They are based on the so-called "entrainment effect" of the vortices. They continuously centrifuge micro turbulence which entrains fresh jet gas into the inner zone and fresh ambient gas into the outer zone of the mixing layer. Thus they retard the turbulent mixing. Such a gas transporting effect may clearly be seen on a calculated video of Kelvin-Helmholtz-Instability published at "www.wikipedia.com". As a result of this gas transport into the mixing layer the sound speeds in the two zones remain practically constant over that length where the Mach waves have constant angles.

The formulation of the velocity u* in equations (12) and (13) needs a consideration of the whole mixing layer as sketched in Fig. 14. The mixing layer cross-section reduces due to suction produced by the vortices. In the system moving with speed u* equal Mach numbers assure equal pressures on both sides of the mixing layer furnishing the following equation:

$$\frac{u_i - u^*}{a_i} = \frac{u^*}{a_a} \quad (14)$$

Comparing equations (10) and (14) we get u* = w. Introducing u* = w in (12), (13) and (14) we obtain:

$$\frac{u_i - w}{a_i} = \frac{w}{a_a} \quad (10) \quad \text{and} \quad \frac{w}{a_a} = \frac{M_i}{1 + a_a/a_i} \quad (11).$$

$$\frac{u_i - w'}{a_i} = \frac{w' - w}{a_a} \quad (15) \quad \text{and} \quad \frac{w'}{a_a} = \frac{M_i + w/a_a}{1 + a_a/a_i} \quad (17)$$

$$\frac{w - w''}{a_i} = \frac{w''}{a_a} \quad (16) \quad \text{and} \quad \frac{w''}{a_a} = \frac{M_i - w/a_a}{1 + a_a/a_i} \quad (18).$$

Many different attempts for explaining the simple empiric formulae (4 - 6) theoretically by gasdynamic considerations had been fruitless for a long time. But with the vortex pair suggestion and the gas entrainment assumption, for the special case $w/a_a = 1$ at which the experimental studies have been undertaken, the theoretical relations (11, 17, 18) correspond exactly to the empirical ones (7 - 9). In order to show how well the equations work, in Fig. 17 the experimentally determined angle α' and the calculated one are indicated with reasonable agreement within the measuring accuracy.

5 Limitations for Mach wave formation

The domain of validity of the formulae given is limited by some Mach number considerations. The w'- and the w''-Mach waves can only exist at the following conditions:

$$w' > a_a \text{ with } M_i > (1 + a_a/a_i)^2 / (2 + a_a/a_i) \quad (19),$$

$$u_i - w'' > a_i \text{ with } M_i > (1 + a_a/a_i)^2 / (1 + 2\,a_a/a_i) \quad (20).$$

Both Mach waves may disappear when one of the two vortices has supersonic relative Mach numbers and at least the regularity can only exist for:

$$w'' < a_a \text{ at } M_i < (a_i/a_a)(1 + a_a/a_i)^2 \quad (21),$$

$$u_i - w' < a_i \text{ at } M_i < (1 + a_a/a_i)^2 \quad (22).$$

Only in the grey domain of Fig. 15 the conditions for regular w'-Mach waves are fulfilled. For test purposes some jet data are introduced in Fig. 15. The free jets in Fig. 16 show no Mach waves and this observation is marked by open circles which are placed outside the borders given by equations (19) and (20). The data of the jet Mach waves seen for example in Figs. 1, 3 and 17 are represented by the solid dots in Fig. 15 and confirm well the lower boundaries (19) and (20). Testing the upper

limitations (21) and (22), experiments show a weak transition in suppressing the Mach wave production by putting more energy into the jet. Exceeding the limits (21) and (22) let the vortex pairs vanish by supersonic overpressures on the bulges.

If the conditions are met for regular Mach waves, then with growing distance from the jet exit the front vortex overtakes the rear vortex of the preceding one for forming one big vortex moving with velocity w. With larger jets having much longer mixing layers such procedures must finally lead to create long chains of jet surrounding vortices travelling at speed w. This might be the domain of considerations like those of Tam et al. [8] and others. Their calculations of waves surrounding a jet without beginning and end are certainly not able to describe the phenomena near the jet exit.

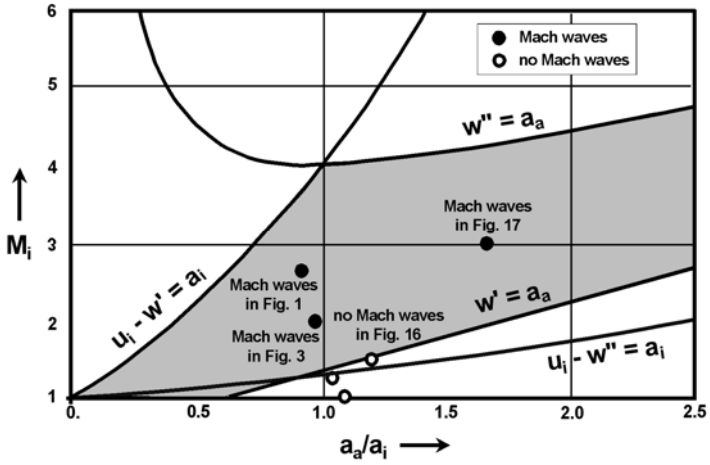

Fig. 15 Range of validity

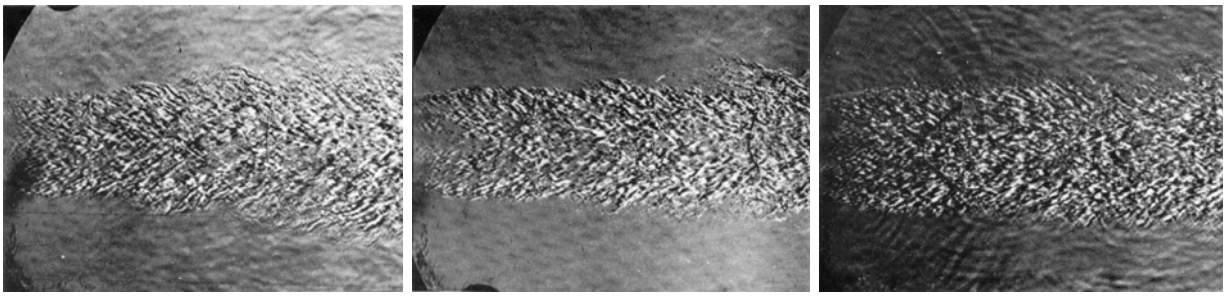

Fig. 16 No Mach waves from free jets with M_j = 1.0, 1.26 and 1.52 (left to right), $a_a/a_i \approx 1$

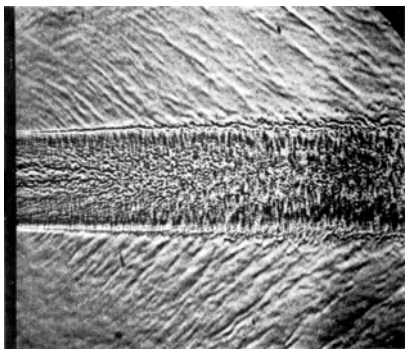

Fig. 17 w'-Mach waves outside of a supersonic free jet with $M_j = 3$, $a_a/a_i \approx 1.64$, $\alpha' \approx 42° \pm 4°$
(theoretical angle using equations (11) and (17): $\alpha' \approx 39.7°$)

References

1. Oertel H. *Coherent structures producing Mach waves inside and outside of the supersonic jet*. IUTAM Symposium on complex structures in turbulent flow. IMST d'Aix-Marseille 1982 and ISL report CO 82/218, 1982
2. Oertel H.. *Kinematik der Machwellen in Überschallstrahlen.* ISL-report R 112/78, 1978
3. Ffowcs J. E. W., Maidanik G. *The Mach wave field radiated by supersonic turbulent shear flows.* Journal of Fluid Mech. 21, 4, pp. 641-657, 1965.

4. Tam C. K. W. *Directional acoustic radiation from a supersonic jet generated by shear layer instability*. Journal of Fluid Mech. Vol. 461, part 4, pp. 757-768, 1971.
5. Poldervaart L. P., Wijands A. P. J. *Sound Pulse-Boundary Layer Interaction Studies*. A. V. Centre, T. H. E., Eindhoven, Netherlands. Private communication, 1974
6. Tam C. K. W. *Supersonic jet noise generated by large scale disturbances*. Journal of Sound and Vibration, 38(1), pp. 51-79, 1975
7. Laufer J., Schlinker R., Kaplan R. E. *Experiments on supersonic jet noise*, AIAA Journal, Vol. 14, No. 4, pp. 489-497, 1976
8. Tam C. K. W., Fang Q. H. U. *On the three families if instability waves of high-speed jets.* Journal of Fluid Mech., Vol. 201, pp 447-484, 1989
9. Tam C. K. W. *Supersonic jet noise*. Annu. Rev. Fluid Mech., 27, pp-17-43, 1995
10. Bailly C., Candel S., Lafon P. *Prediction of supersonic jet noise from a statistical acoustic model and a compressible turbulence closure*. Journal of Sound and Vibration, Volume 194, Issue 2, 1996
11. Papamoschou D., Bunyajitradulya A. *Evolution of large eddies in compressible shear layers*. Physics Fluids 9(3), 1997
12. Papamoschou D. *Mach wave elimination in supersonic jets*. AIAA-97-0147, 1997
13. Colonius T., Lele S. K., Moin P. *Sound generation in a mixing layer*. Journal Fluid Mech., vol. 330, p.p. 375-409, 1997
14. Papamoschou D., Debiasi M. *Noise measurements in supersonic jets treated with the Mach wave elimination method*. AIAA Journal, Vol. 37, No. 2, 1999
15. Lele S. K., Mendez S., Ryu J., Nichols J., Shoeybi M., Moin P. *Sources of high-speed jet noise: analysis of LES data and modeling*. Procedia Engineering 6C, pp. 84-93, 2010
16. Freund J. B., Lele S. K., Moin P. *Numerical simulation of a Mach 1.92 turbulent jet and its sound field.* AIAA J., Vol. 38, No. 11, 2000
17. Rossmann T., Mungal M. G., Hanson R. K. *Character of Mach wave radiation and convection velocity estimation in supersonic shear layers.* AIAA 2002-2571, 2002
18. Bassetti A. *A statistical jet-noise model based on the acoustic analogy and a RANS solution.* University of Southampton, Institute of Sound and Vibration Research, Doctoral thesis, 2009
19. Oertel H. *Jet noise research by means of shock tubes*. Proc. of the 10th Int. Shock Tube Symp. Japan, Kamimoto, 1975
20. Oertel H. *Mach wave radiation of hot supersonic jets investigated by means of a shock tube and new optical techniques*. In Proc. 12. International Symposium on shock-tubes and waves, Jerusalem, 1980
21. Oertel H. *Measured velocity fluctuations inside the jet boundary layer of a Supersonic je.*, In Recent contributions to fluid mechanics, Springer Berlin, 1982
22. Oertel H. *33 years of research by means of shock tubes at the French-German Research Institute of Saint-Louis*. Proc. 14th International Symposium on Shock Tubes and Waves, pp. 3-13, Sydney, Archer Milton, 1983
23. Oertel sen. H., Seiler F., Srulijes J. *New explanation of noise production by supersonic jets with gas dredging*. Notes on Numerical Fluid Mechanics and Multidisciplinary Design, Vol. 112, Springer-Verlag Berlin Heidelberg, 2010
24. Oertel sen. H., Seiler F., Srulijes J. *Vortex induced Mach waves in supersonic jets*. Proceedings of the 28th International Symposium on Shock Waves ISSW28, Manchester, July 2011, 2011
25. Oertel sen. H., Oertel jun. H. *Optische Strömungsmesstechnik*. Braun-Verlag, Karlsruhe, 1989
26. Oertel H. *Stossrohre*. Springer, Wien 1966
27. Srulijes J., Seiler F. *A review of some flow visualization experiments carried out at the ISL shock tubes*. Flow Visualization IV, Springer-Verlag Berlin, 1987